# Higher-Order Interactions in Auxotroph Communities Enhance Their Resilience to Resource Fluctuations

Tong Wang[1,2], Ashish B. George[2,3,4], Sergei Maslov[1,2,5,*]

[1] *Department of Physics, University of Illinois at Urbana-Champaign, Urbana, IL 61801, USA.*
[2] *Carl R. Woese Institute for Genomic Biology, University of Illinois at Urbana-Champaign, Urbana, IL 61801, USA.*
[3] *Department of Plant Biology, University of Illinois at Urbana-Champaign, Urbana, IL 61801, USA.*
[4] *Broad Institute of MIT and Harvard, Cambridge, MA 02142, USA.*
[5] *Department of Bioengineering, University of Illinois at Urbana-Champaign, Urbana, IL 61801, USA.*

[*] Correspondence to: `maslov@illinois.edu`
(Dated: May 17, 2024)

Auxotrophs are prevalent in microbial communities, enhancing their diversity and stability—a counterintuitive effect considering their dependence on essential resources from other species. To address the ecological roles of auxotrophs, our study introduced a novel consumer-resource model that captures the complex higher-order interactions within these communities. We also developed an intuitive graphical and algebraic framework, which assesses the feasibility of auxotroph communities and their stability under resource fluctuations and biological invasions. Validated against experimental data from synthetic *E. coli* auxotroph communities, the model accurately predicted outcomes of community assembly. Our findings highlight the critical role of higher-order interactions and resource dependencies in maintaining the diversity and stability of microbial ecosystems dominated by auxotrophs.

## INTRODUCTION

Auxotrophs, organisms that cannot synthesize essential resources and are therefore forced to rely on their production by other species, are extremely common in microbial communities[1–4]. Despite the vulnerability of individual auxotrophic species to essential resource deprivation, research shows that communities with high proportions of auxotrophs exhibit increased diversity and stability[5]. This raises intriguing questions about the ecological and evolutionary benefits of auxotrophy, a topic that has not been quantitatively explored in mechanistic models.

Traditional models, which assume that growth rates of auxotrophs depend linearly on the abundances of other species that synthesize missing essential resources, do not adequately capture the complex dynamics within auxotroph communities[6,7]. For example, a generalized Lotka-Volterra (gLV) model, which focuses on such pairwise interactions, completely failed to predict the assembly outcome of a community of 14 *E. coli* synthetic auxotrophic strains[8]. In fact, it predicted the coexistence of all 14 strains, while only 4 strains survived in experiments. The growth of auxotrophs is described by Liebig's law of minimum, which in turn depends on the concentrations of many essential resources (e.g., 20 amino acids). This results in significant higher-order interactions between species[9,10] and underscores the need for a more sophisticated modeling approach than the pairwise gLV model.

In this study, we use the Consumer-Resource Modeling (CRM) framework[11,12], which more accurately represents resource concentrations and acquisition mechanisms. We introduce and study a novel consumer-resource model of auxotroph communities that goes beyond simple pairwise interactions and captures essential higher-order interactions and resource dependencies. Each species in our model is capable of transforming the primary resource (e.g., glucose) into multiple essential resources (e.g., amino acids), a capability that auxotrophs lack for some resources. Thus, our model can account for both auxotrophic and prototrophic species.

We also develop an intuitive graphical and algebraic framework that assesses the feasibility of auxotroph communities and their stability under resource fluctuations and biological invasions by other species. Our approach offers insights into complex interactions and resource strategies in auxotroph communities. Its success is highlighted by a successful prediction of 3 out of 4 surviving strains and extinction of the remaining 10 strains in communities of *E. coli* synthetic auxotrophic strains.

## MODEL AND RESULTS

### Consumer Resource Model of Auxotroph/Prototroph Microbial Communities

We aim to model a general situation in which microbial strains are capable of transforming (green arrows in Fig. 1a) a single externally supplied carbon source (e.g., glucose) into multiple essential resources (e.g., amino acids). We assume that a fraction of essential resources is stoichiometrically transformed to biomass (red arrows in Fig. 1a), while the rest overflows into the environment (orange arrows in Fig. 1a). We also assume that all species

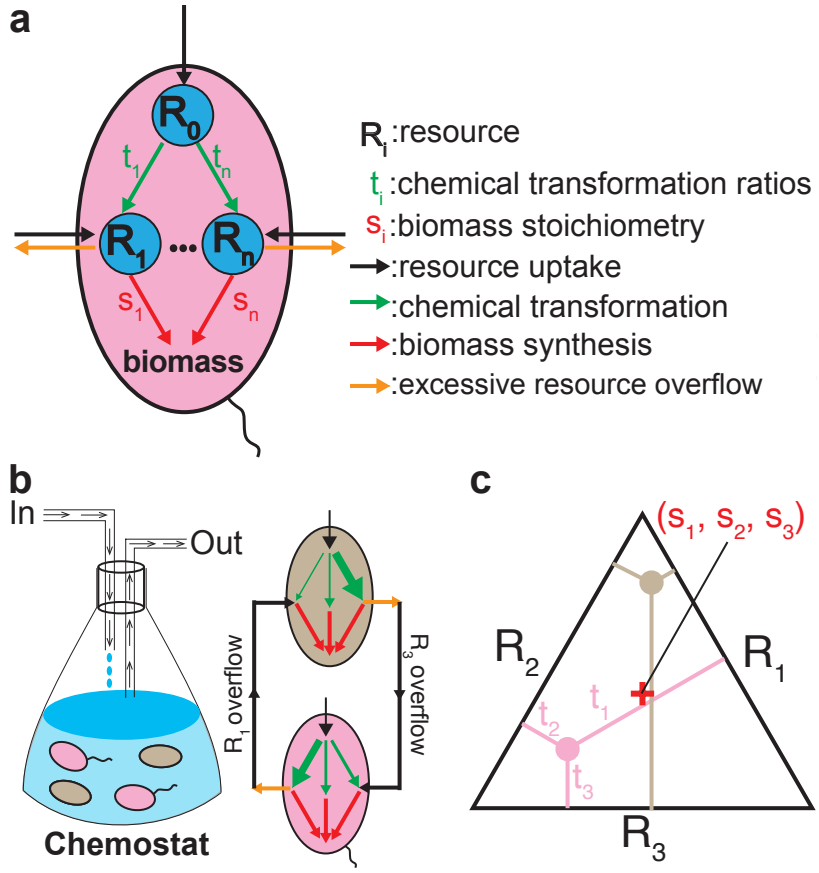


FIG. 1. **Conversion and exchange of resources in our model of auxotroph communities.** **a** Schematic illustration of intracellular processes in one species. Each species is capable of transforming a primary resource $R_0$ (e.g., glucose) into a subset of other resources ($R_1$,...,$R_n$) essential for growth (e.g., amino acids). Different species have unique transformation vectors $\vec{t}$ quantifying this conversion but share the same biomass stoichiometry $\vec{s}$. If the transformation flux of an essential resource (green arrows) exceeds its flux directed to biomass (red arrows), the excess is secreted as the overflow flux (orange arrows). Otherwise, a microbe can uptake essential resources directly from the environment (black arrows) to balance its biomass synthesis flux. **b** Depiction of a microbial community in a chemostat (red arrows). The pink microbe uptakes $R_3$ and produces $R_1$ due the exssive transformation of $R_1$. The green-grey microbe uptakes $R_1$ and produces $R_3$. As a result, two microbial species cooperate via exchange of essential metabolites. **c** Graphical representation of the microbial community (panel b) in the resource simplex when $\sum_i t_i^{(\alpha)} = 1$. Two species, represented as pink and brown dots inside a simplex, have identical biomass stoichiometry $\vec{s} = (1, ..., 1)$ but different transformation fluxes. The distances from a species' position inside a simplex to its three sides are proportional to its corresponding transformation fluxes ($t_1$, $t_2$, and $t_3$). The red cross at the simplex's center represents the shared stoichiometry vector.

can freely use overflow resources released by other species (black arrows in Fig. 1a). Lastly, we assume that the stoichiometry in which essential resources are used for biomass synthesis is the same across all species.

In mathematical notation, the fluxes transforming one unit of the primary resource (green arrows in Fig. 1a) into multiple essential resources ($R_i$ with $i = 1 : n$ in Fig. 1a) are represented as a transformation vector $\vec{t}^{(\alpha)} = (t_1^{(\alpha)}, ..., t_n^{(\alpha)})$ (green arrows in Fig. 1a). Thus the transformation flux at which species $\alpha$ generates essential resource $i$ is modeled as $t_i^{(\alpha)} R_0$, where $R_0$ is the concentration of the primary resource. All species share the same biomass synthesis stoichiometry, denoted by $\vec{s} = (s_1, ..., s_n)$ (red arrows in Fig. 1a). This assumption is supported by similar amino acid compositions of microbial biomass across various species[13–15]. By changing the units of concentration of different amino acids, we can make this universal stoichiometry to be given by $\vec{s} = (1, \ldots, 1)$. Microbes also uptake essential resources $R_i$ from their environment (black arrows in Fig. 1a), with the uptake rate proportional to $R_i$. Assuming a passive exchange of essential resources between species and the environment, without loss of generality, we can set the maximal uptake rate from the environment as $R_i$, which is the same for each species. Thus, the maximal total flux of the essential resource $i$ for species $\alpha$ that could in principle be converted to the biomass is given by $F_i^{(\alpha)} = t_i^{(\alpha)} R_0 + R_i$. This expression accounts for both

the intracellular transformation of the primary resource and the direct uptake of $R_i$ from the environment.

The growth of microbes follows Liebig's law of the minimum, positing that growth is constrained by a single limiting essential resource[16,17]: the specific growth rate $g^{(\alpha)} = \min(\frac{F_1^{(\alpha)}}{s_1}, ..., \frac{F_n^{(\alpha)}}{s_n})$. If resource $i$ is the limiting resource of species $\alpha$, then for resource $j$, the flux used for biomass synthesis is $\frac{s_j}{s_i} F_i^{(\alpha)}$ (red arrows in Fig. 1a), and the remaining flux (i.e., $F_j^{(\alpha)} - \frac{s_j}{s_i} F_i^{(\alpha)}$) is the overflow flux (orange arrows in Fig. 1a). We then model the population dynamics within a chemostat environment, characterized by constant resource supply rates and fixed dilution rates for both species and resources (Fig. 1b).

### Graphical interpretation of the feasibility and stability criteria

If the transformation efficiency of the primary resource is the same across all species, the transformation vector can be normalized so that $\sum_i t_i^{(\alpha)} = 1$. When applying our model to actual data on auxotrophic strains of *E. coli*, we will relax this assumption. In scenarios involving three essential resources, each species can be represented as a point within an equilateral triangle (pink and brown dots on a three-dimensional simplex in Fig. 1c). The distances from the species' position to the simplex's three sides ($t_1$, $t_2$, and $t_3$) are proportional to its capacity to transform the primary resource $R_0$ to essential resources $R_{i(\geq 1)}$ respectively. Similarly, the stoichiometry vector $\vec{s} = (1, ..., 1)$ is depicted as the red cross at the center of the equilateral triangle (Fig. 1). These graphical representations, along with subsequent analysis, will be extended to cases where species differ in their transformation efficiencies.

In ecosystems, achieving a stable steady state hinges on two key criteria: feasibility[18] and stability[19,20]. A state is deemed feasible if all surviving species have zero net growth rates and maintain non-negative abundances at the steady state[18]. For our model, we modified this concept by defining "flux feasibility" for the full-diversity communities, which is determined by whether the stoichiometry vector (the red cross in Fig. 2a) lies within the convex hull formed by the species' transformation vectors $\vec{t}^{(\alpha)}$ (yellow triangle in Fig. 2a). If the stoichiometry vector falls outside the yellow triangle, the coexistence among the three species is not feasible (Fig. 2b). This feasibility criterion can also be expressed using linear algebra, which is particularly useful in high-dimensional cases (Supplementary Fig. 1). We define the "community transformation vector" $\vec{C} = \sum_\alpha N_\alpha \vec{t}^{(\alpha)}$, where $N_\alpha$ is the relative respective abundance of species $\alpha$. $\vec{C}$ gives the average transformation flux of the community and constructs the convex hull (yellow triangle in Fig. 2a). The feasibility domain encloses the stoichiometry vector $\vec{s}$, indicating that $\vec{C}$ can align with $\vec{s}$ by adjusting species abundances. Mathematically, a full-diversity community is achievable if $\vec{C} = \vec{s}$. Details of the algebraic analysis for communities with sub-maximal diversity are provided in Supplementary Fig. 1.

In ecological models involving multiple essential resources, a species' growth rate is typically determined by a single growth-limiting resource[21,22]. In our model, for a given essential resource $R_i$, the species with the least capacity to produce it on its own must uptake more of it from the environment than other species, thereby becoming growth-limited by this resource. To illustrate this, let us consider a case with three essential resources and three species (Fig. 2c). Geometrically, the species that is growth-limited by a specific resource is the one whose position within the simplex is the closest to the side representing this resource. For instance, in Fig. 2c, species $\beta$ is closest to the triangle's bottom side, indicating that it is growth-limited by resource $R_3$. Similarly, species $\alpha$ and $\gamma$ are limited by resources $R_2$ and $R_1$, respectively. More generally, in a maximally diverse ecosystem with the number of species equal to the number of resources, each species's growth is limited by a unique resource, and each resource limits the growth of one species only[22]. This principle holds for the community in Fig. 2c, confirming its "competitive stability". Conversely, the community shown in Fig. 2d is not competitively stable since the growth of species $\theta$ is limited by both $R_1$ and $R_3$.

This observation allows us to introduce an "Invasion Boundary" (IB), a line (or more generally a hyperplane) drawn through each species' position within a simplex and parallel to the side representing its growth-limiting resource. Any potential invader species positioned closer to the resource than the IB cannot successfully invade the community. Indeed, for such a species, the concentration of this resource will be insufficient for exponential growth in our chemostat. Conversely, an invader species located further away from all resources than surviving species' IBs (species within the blue triangle in Fig. 2c) will succeed in invading this community. This theoretical prediction was confirmed by our numerical simulations of $\sim 500$ attempted invasions of this community by random invader species (successful/failed invasions as blue/grey dots in Fig. 2e).

The scenario in Fig. 2d is inherently unstable, and one can show that species $\iota$ would eventually outcompete $\eta$ (Supplementary Fig. 1). Two surviving species, $\theta$ and $\iota$, will be growth-limited by $R_1$ and $R_2$ correspondingly (see detailed algebraic analysis in Supplementary Fig. 1). As before, we predict that successful invaders have transformation vectors inside the region formed by IBs of surviving species ($\theta$ and $\iota$) in the community, while unsuccessful invaders have transformation vectors outside this region. This theoretical prediction is corroborated by numerical simulations shown in Fig. 2f, where the IBs for the two surviving species separate successful invaders (blue dots) from unsuccessful ones (grey dots) among $\sim 500$ attempted invasions.

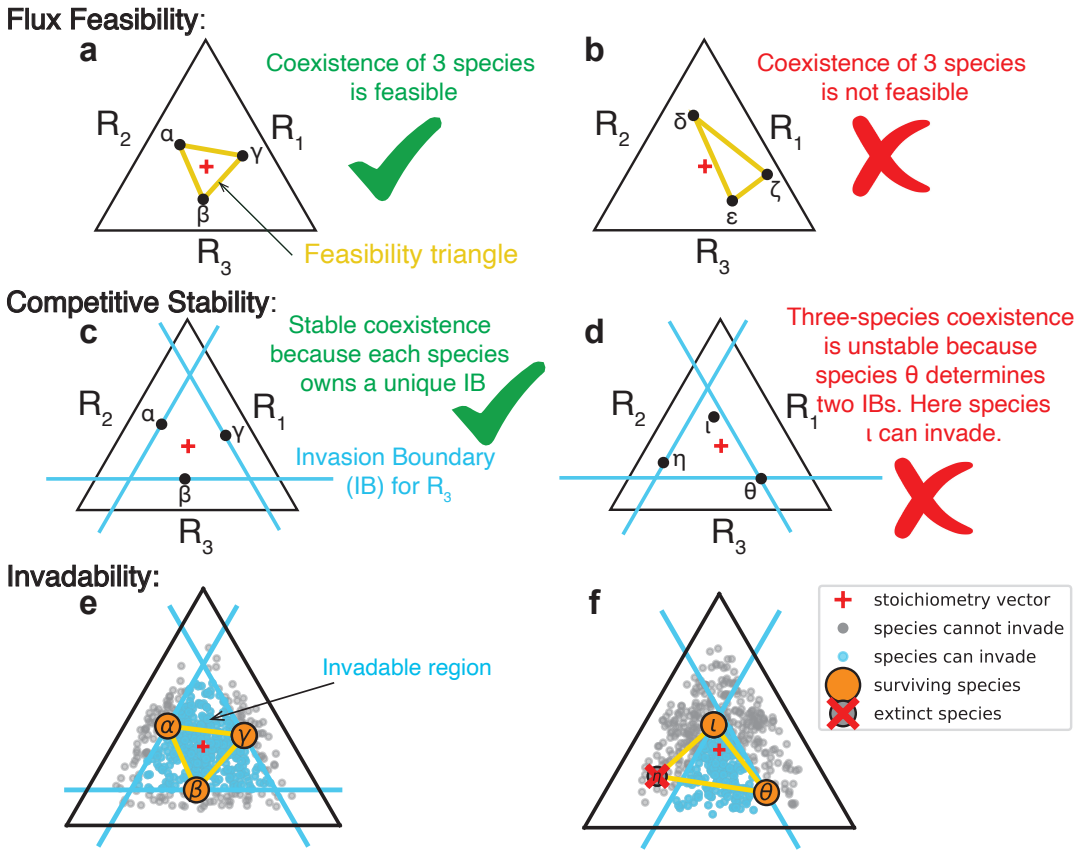


FIG. 2. **Graphical interpretation of flux feasibility and competitive stability. a-b** The flux feasibility of a full-diversity community depends on whether the stoichiometry vector is within the convex hull formed by connecting transformation vectors of all species (yellow feasibility triangle). **c-d** The competitive stability of a full-diversity community depends on whether each species is growth-limited by a unique resource. For each essential resource, the species growth-limited by it has the weakest transformation capability for the resource and needs to uptake the resource most from the environment, thereby determining the IB (Invasion Boundary) that is a line drawn through the species' position within a simplex and parallel to the side representing its growth-limiting resource. **e-f** Model simulations demonstrate the invadability. The invadable region is bounded by IBs. These simulations start a community assembly with three species (labeled in each panel) in a chemostat, allowing it to reach a stable steady state. Invasion simulations, conducted 497 times, involve introducing a single species with a randomly chosen transformation vector into the steady state to test its ability to invade the community. Successful and failed invasions are marked with light blue and grey dots, respectively.

### Model with externally supplied essential resources and different conversion efficiencies

Until now, our analysis has assumed that the primary resource $R_0$ was the only external supply to the ecosystem. In this case, the only source for essential resources $R_i$ was the transformation of $R_0$ by species in the community. However, in natural ecosystems, some essential resources may be directly supplied. Our methods for evaluating flux feasibility and competitive stability can be easily extended to this scenario. Externally supplied resources are modeled by a vector, $\vec{t}^{\text{ext}}$, whose $i$'s component is the ratio of the external supply rate of the essential resource $R_i$ to that of the primary resource $R_0$ (Supplementary Fig. 2a). As a result, the community transformation vector becomes $\vec{C} = \sum_\alpha N_\alpha \vec{t}^{(\alpha)} + \vec{t}^{\text{ext}}$, combining the collective transformation of $R_0$ into $R_i$ with the direct supply of $R_i$. For a maximally diverse community in steady state, the community transformation vector must be equal to the stoichiometry vector $\sum_\alpha N_\alpha \vec{t}^{(\alpha)} + \vec{t}^{\text{ext}} = \vec{s}$. The condition for flux feasibility thus becomes $\sum_\alpha N_\alpha \vec{t}^{(\alpha)} = \vec{s} - \vec{t}^{\text{ext}}$ with positive $N_\alpha$. Geometrically, this is depicted as a shift of the stoichiometric vector from $\vec{s}$ to $\vec{s} - \vec{t}^{\text{ext}}$ (red star inside a simplex in Supplementary Fig. 2a). The community is feasible provided that this shifted stoichiometry vector $\vec{s} - \vec{t}^{\text{ext}}$ lies within the convex hull formed by $\sum_\alpha N_\alpha \vec{t}^{(\alpha)}$, validated by numerical simulations shown in Supplementary Fig. 2.

We also adapted our graphical and algebraic methods to the situation when species do not fully transform the primary resource $R_0$ to essential resources $R_i$, resulting in different overall conversion efficiencies ($\sum_i t_i^{(\alpha)} < 1$). We demonstrated this model variant with a system of

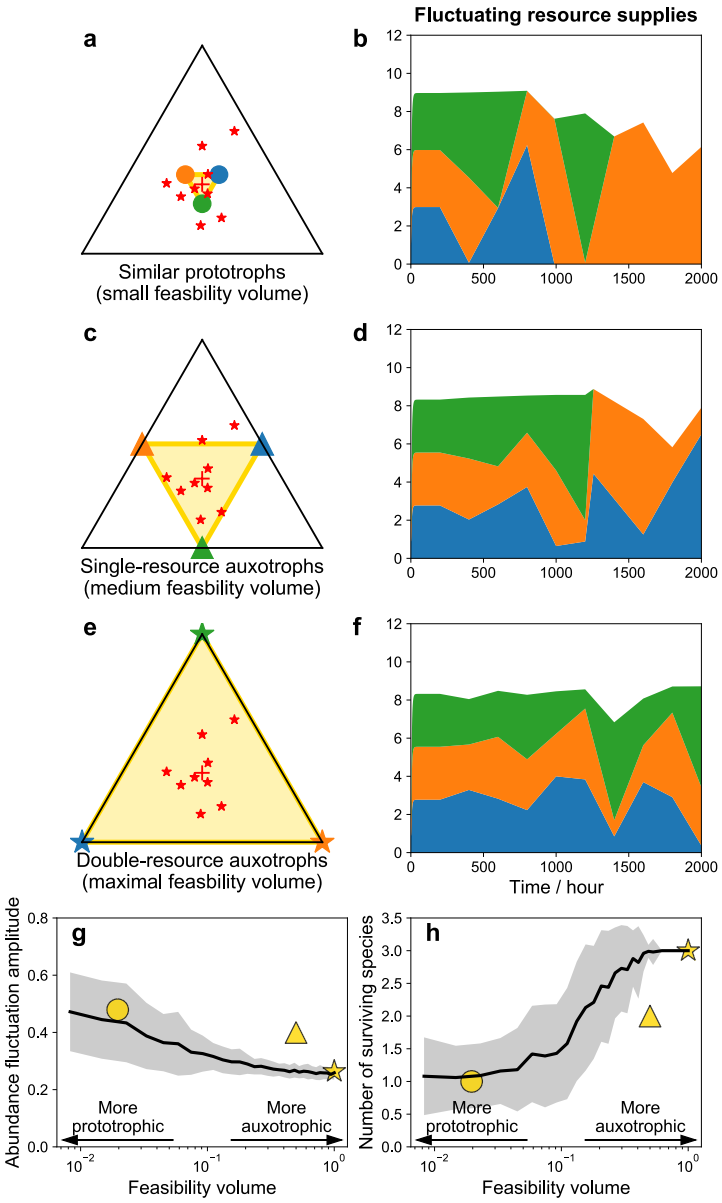


FIG. 3. **Auxotroph communities are more resilient to resource fluctuations.** In these simulations, fluxes of essential resources externally supplied to the system change every 200 hours, with each change gradually increasing in magnitude. The red stars represent $\vec{s} - \vec{t}^{\text{ext}}$ after each such change. **a** A community of three prototrophs with similar transformation abilities. **b** The dynamics of the community composition shown in panel a under fluctuating supply of essential resources. **c** A community of three single-resource auxotrophs. **d** The compositional dynamics of the community shown in panel c. **e** A community of three double-resource auxotrophs. **f** The compositional dynamics of the community shown in panel e. **g** The average magnitude of fluctuations in microbial abundances, defined as the standard deviation of time-series abundances divided by their mean, decreases as the feasibility volume increases from prototrophs to double-resource auxotrophs. **h** The average richness of assembled communities increases with the feasibility volume. Simulations in panels e and f are averaged over 100 repeats for each bin of feasibility volumes. The black line represents the mean values of the y-axis and the grey area represents one standard deviation from the mean. Simulations shown in panels a-f are indicated by the corresponding symbols: circle for prototrophs in panel a, triangle for single-resource auxotrophs in panel c, and star for double resource-auxotrophs in panel e.

2 essential resources and 2 species (Supplementary Fig. 3). Our graphical and algebraic approach remains applicable in this general case. For the community shown in Supplementary Fig. 3, we predict the coexistence of the two species since they satisfy (1) the flux feasibility condition: each species is positioned on opposite sides of the $y = x$ line defined by the stoichiometry vector (1,1) (Supplementary Fig. 3a) and (2) the competitive stability condition: each species has a unique limiting resource (Supplementary Fig. 3a). The outcome of our

invasion simulations validated the prediction based on our graphical method (invadable region with blue dots in Supplementary Fig. 3c).

### Auxotroph communities are more resilient to resource fluctuations

Why is auxotrophy so widespread in natural communities? What advantage could there be for a prototrophic species, capable of synthesizing all essential resources for its growth, to lose this ability to produce one or more resources? Our model suggests a possible answer to these questions. By comparing the relatively small feasibility volume of communities populated by prototrophic species (small yellow triangle in Fig. 3a) to the progressively larger feasibility volumes of communities composed of single-resource auxotrophs (medium yellow triangle in Fig. 3c) and double-resource auxotrophs (largest possible yellow triangle in Fig. 3e), we conclude that auxotrophy may enhance community survival in environments with fluctuating external supplies of essential resources. Our graphical approach illustrates that changes in the external supply of essential resources manifest as shifts in the vector $\vec{s}$. Communities with a larger feasibility domain are better equipped to handle these shifts, as all community species can survive as long as the shifted vector $\vec{s} - \vec{t}^{\text{ext}}$ remains within the feasibility domain.

To verify this intuition, we studied the dynamics of three communities under conditions of fluctuating essential resource supplies, each with varying feasibility volumes: (1) communities with similar prototrophic species (Figs. 3a-b), (2) communities of single-resource auxotrophs with medium feasibility volume (Figs. 3c-d), and (3) communities comprising double-resource auxotrophs with maximal feasibility volume (Figs. 3e-f). We modeled these fluctuations by independently and uniformly sampling the ratio of the supply rate of each essential resource to that of the primary resource ($t_i^{\text{ext}}$) between 0 and 0.3 every 200 hours.

When three prototrophic species with similar transformation abilities face fluctuations in essential resource supplies (Fig. 3a-b), their species abundances fluctuate dramatically. In a representative simulation shown in Fig. 3b, the blue and green species die out after 1400 hours due to resource fluctuations. In contrast, in a community of three single-resource auxotrophs (Fig. 3c-d), three species manage to coexist longer, with two surviving even after 2000 hours. The community composed of three double-resource auxotrophs has the largest possible feasibility volume, so in a representative simulation of this community shown in Fig. 3f, all three species survived indefinitely. We systematically explored how the feasibility volume impacts the abundance fluctuation and the richness of the assembled community. By measuring 'abundance fluctuation amplitude' through the ratio of the standard deviation to the mean of species abundances, we observed a consistent decrease in abundance fluctuation amplitude with increasing feasibility volume (Fig. 3g). This decrease reduces the likelihood of species extinction, thereby enhancing community richness and stability (Fig. 3h).

### Accurate predictions of experimentally assembled auxotroph communities

To showcase our model's capability in predicting community assembly outcomes, we applied it to experimental data from a synthetic community comprised of 14 *E. coli* auxotroph strains, each genetically engineered to lack the ability to synthesize one specific amino acid[8]. This synthetic community was investigated through (1) pairwise co-cultures of auxotroph pairs (91 pairs in total, 1 replicate each pair) and (2) a co-culture of all 14 auxotrophs (2 replicates). We first fitted the transformation vectors for these auxotrophs using fold-growth observed in pairwise co-culture growth experiments (Fig. 4a). Using these fitted vectors, we then predicted the assembly outcome of the community comprising all auxotrophs. Instead of fitting the stoichiometry vector, we used the previously reported biomass composition of amino acids in *E. coli*[8].

We iteratively adjusted the transformation vectors for each of the 14 strains across every amino acid ($14 \times 13 = 182$ parameters since each synthetic auxotroph strain is unable to synthesize one amino acid, which results in its transformation value of zero for that amino acid). The fitting used the data on fold-growth in 91 pairwise co-culture experiments (Supplementary Fig. 4). Note that we use the version of our model that allows for the incomplete transformation of the primary resource ($\sum_i t_i^{(\alpha)} < 1$). To illustrate our iterative algorithm, let us consider a co-culture of $\Delta T$ and $\Delta M$ strains. If the fold-growth of $\Delta T$ predicted by our model exceeds or falls short of the experimental value, we adjust $\Delta M$'s transformation ability of $T$ upward or downward respectively to minimize the discrepancy (Supplementary Fig. 4). This process is repeated until we obtain the best-fitted transformation vectors (Fig. 4b and Supplementary Fig. 6).

Using these fitted transformation vectors, our model accurately predicted three species out of four surviving species observed experimentally ($\Delta K$, $\Delta M$, and $\Delta T$ in Fig. 4a) and the extinction of the remaining 10 species. For comparison, we applied the previously proposed gLV model[8], which has the same number of fitting parameters (182) as our model and used the same pairwise co-culture data for fitting (see Methods for more details). Although the gLV model fitted pairwise co-culture data better (Supplementary Fig. 5), it completely failed in selecting which species would survive in the full community assembly. Indeed, the gLV model predicted the survival for all 14 species, diverging significantly from experimental observations with only four survivors (gLV results in Fig. 4a). This spectacular failure of the gLV model, which only accounts for pairwise interactions, indicates the importance of higher-order interactions in auxotroph

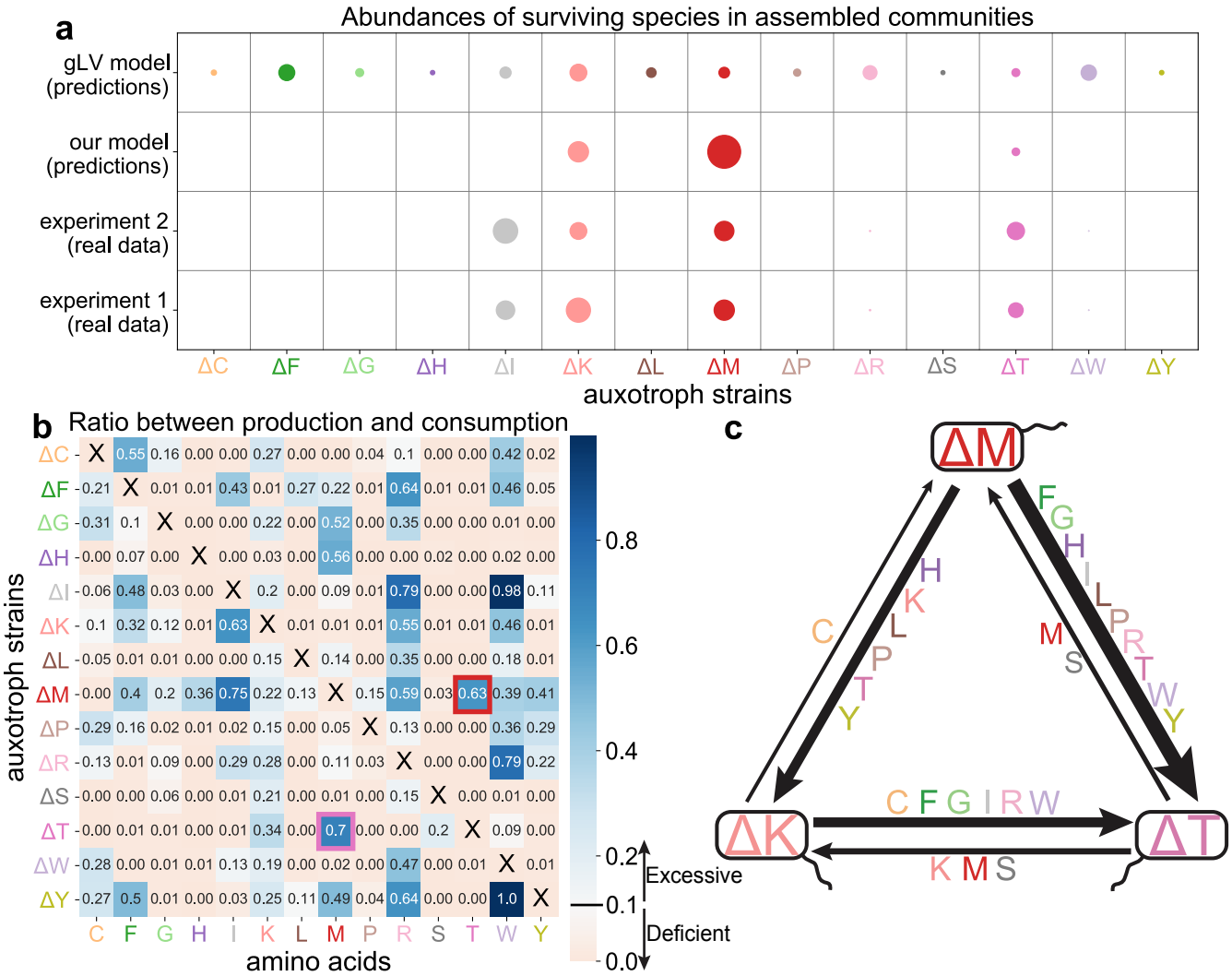


FIG. 4. **Our model prediction of the community assembly inoculated by 14 *E. coli* synthetic auxotrophs.** Color assignments for all species and amino acids are consistent across all panels. The full names of amino acids are listed in the Methods section. The prefix Δ indicates a single amino acid auxotrophy (e.g., $\Delta T$ refers to the strain unable to synthesize Threonine (T)). **a** Our model's prediction of the steady state composition for the full diversity 14-member assembly (second line) closely matches the experimental results (two biological replicates shown in lines 3 and 4) by correctly predicting three out of four surviving species. Conversely, the generalized Lotka-Volterra (gLV) model fitted to the pairwise assembly data (first line) incorrectly predicts the survival of all 14 species. **b** The ratio of the best-fitted transformation vector in our model to the stoichiometry vector experimentally measured in *E. coli*. The synthetic resource auxotrophy for each strain is marked with ×. Red and purple squares mark the only pair of strains ($\Delta M$ and $\Delta T$) with a strong (> 0.5 for each strain) mutual exchange flux of amino acids (T and M) they cannot produce. **c** The exchange fluxes of amino acids between three surviving species predicted by our model.

communities.

The fitted transformation vectors enable us to accurately map the niche of each auxotroph within the resource space, identify strong competitors, and identify the most effective mutualistic pairs or trios (Fig. 4b). Notably, the strain $\Delta T$ emerges as the ideal mutualistic partner for the strain $\Delta M$, due to the surplus production of $M$ by $\Delta T$ (the purple square in Fig. 4b) and abundant production of $T$ by $\Delta M$ (the red square in Fig. 4b). Note that $\Delta T$ and $\Delta M$ are the only pair of auxotrophic strains that each produces the other strain's missing amino acid in sufficient quantities: $\frac{t_i^{(\alpha)}}{s_i} > 0.5$. We further summarized the exchange of amino acids between surviving strains using a graph (Fig. 4c), revealing that $\Delta M$ is a key supplier of most amino acids to both $\Delta K$ and $\Delta T$. Meanwhile, $\Delta K$ provides two other strains with cysteine (C), which neither of them can synthesize in adequate amounts.

## Discussion

The role of auxotrophic species in shaping ecological dynamics and community assembly has been underexplored in mechanistic models. In this study, we introduced an innovative ecological model that incorporates both the catabolic and anabolic processes of auxotrophic and prototrophic species, as well as their interactions with the environment. This model provides both graphical and algebraic interpretations of flux feasibility, emphasizing the community's strategies to optimize species abundances to minimize essential resource overflow. It elucidates why auxotroph communities are more diverse and resilient to resource fluctuations. For competitive stability in such optimized communities, species must occupy distinct niches characterized by non-overlapping limiting resources. Applied to experimental data from a synthetic community of *E. coli* auxotroph strains, our model successfully predicted the survival of three out of four strains observed.

Previous attempts to quantitatively understand interactions between auxotrophs have primarily utilized gLV models[8]. However, these models completely failed to predict the assembly of a diverse 14-strain community. This failure arises because gLV models fitted to pairwise data capture only cooperative interactions, due to the mutually beneficial exchange of missing amino acids. Consequently, all interaction coefficients inferred from such models are positive. When such a model is applied to describe a full-diversity community, it erroneously predicts the survival of all strains. A more realistic approach necessitates incorporating both negative, competitive interactions and accounting for complex higher-order effects. Our model addresses these shortcomings by introducing concepts such as competitive stability, invasion boundaries, and growth-limiting resources. These elements not only capture the competition between species but also highlight the potential for one species to drive another to extinction, thereby offering a more nuanced and realistic view of species interactions and community dynamics.

Traditional consumer-resource models[12,21–23] have another deficiency: they usually neglect the details of intracellular metabolism. In contrast, our model offers a coarse-grained yet realistic description of intracellular metabolic transformations, transforming a primary resource (e.g., glucose) into multiple metabolites essential for biomass production (e.g., amino acids), akin to flux balance analysis (FBA)[24,25]. However, our model diverges from FBA by not focusing on maximizing each species' growth rate. Instead, it emphasizes the cooperative sharing of essential resources and balances their overall production and consumption fluxes only at the community level (i.e., flux feasibility). Our model also accounts for the competition between species for niches defined by growth-limiting resources.

Additionally, our model provides insights into the prevalence of auxotrophs in natural communities[1–4], clarifying their role in enhancing community stability[5]. By relying on external sources for essential nutrients, auxotrophs foster interdependence among species, serving as a stabilizing force within the community. We model this interdependence by matching the excess production with the growth limitations of the surviving species. When the external supply of resources shifts, auxotrophic species in our model adjust their populations to buffer these fluctuations, thereby mitigating the impact of changes in resource availability. Thus, communities rich in auxotrophs often display greater ecological resilience and stability compared to those dominated by prototrophs.

## METHODS

**Datasets.** The experimental pairwise and 14-member cocultures of *E. coli* auxotroph strains can be found in the Supplemental Information of Mee et al[8]. The abbreviations of amino acids are as follows: Arginine (R), Cysteine (C), Glycine (G), Histidine (H), Isoleucine (I), Leucine (L), Lysine (K), Methionine (M), Phenylalanine (F), Proline (P), Serine (S), Threonine (T), Tryptophan (W), and Tyrosine (Y).

**The ecological model with production and overflow of essential resources.** Our model considers the depletion, transformation, uptake, and overflow of resources as well as the growth of microbes. For microbial species $\alpha$, it consumes the sole primary resource $R_0$ and then transforms it into essential resources $R_{i(\geq 1)}$. As a result, the transformation flux for essential resource $i$ by species $\alpha$ is $t_i^{(\alpha)} R_0$, where $R_0$ is the concentration of the primary resource and $t_i^{(\alpha)}$ is the rate at which the primary resource $R_0$ is transformed to essential resource $i$. Additionally, species $\alpha$ can uptake resource $i$ directly from the environment, with its uptake flux proportional to $R_i$. Assuming that microbial species passively uptake all essential resources at the same rate, we set the uptake resource as $R_i$. The total influx of essential resource $i$ is given by $F_i^{(\alpha)} = t_i^{(\alpha)} R_0 + R_i$.

The specific growth rate of species $\alpha$ is described by Liebig's law of the minimum: $g^{(\alpha)} = \min(\frac{F_1^{(\alpha)}}{s_1}, ..., \frac{F_n^{(\alpha)}}{s_n})$ where $s_i$ is the stoichiometric fraction of essential resource $i$ required for the biomass synthesis. If the influx of resource $i$ for species $\alpha$ exceeds its rate consumed for biomass synthesis (i.e., $F_i^{(\alpha)} > g^{(\alpha)} s_i$), the unconsumed part forms the overflow flux (i.e., $F_i^{(\alpha)} - g^{(\alpha)} s_i$). The dynamics of species abundances (denoted as $N_\alpha$) and resource concentrations are described by the following equations:

$$\frac{dN_\alpha}{dt} = g^{(\alpha)} N_\alpha - D N_\alpha,$$

$$\frac{dR_i}{dt} = \sum_\beta N_\beta \left( F_i^{(\beta)} - g^{(\beta)} s_i \right) + D R_i^{(0)} - D R_i,$$

where $D$ is the dilution rate and $R_i^{(0)}$ is the pool concentration of resource $i$.

For simulations involving fluctuations in essential resources, the ratio $\frac{R_i^{(0)}}{R_0^{(0)}}$ for each essential resource $i > 0$ is randomly sampled from a uniform distribution between 0 and 0.3 every 200 hours. Regarding the data with 14 *E. coli* auxotroph strains[8], fold-growth observed in pairwise co-cultures is used to fit $t_i^{(\alpha)}$. Eventually, the fitted parameters are used to predict the assembly outcome for the 14-member co-culture.

**The gLV model and its fitting.** The gLV model we utilized is from the mathematical model proposed in Mee et al[8]. In this

model, the abundance dynamics of species $\alpha$ is specified as

$$\frac{dN_\alpha}{dt} = \sum_{\beta \neq \alpha} C_{\alpha,\beta} N_\beta \left(\frac{N_\alpha}{N_\alpha + b}\right)\left(1 - \frac{\sum_\gamma N_\gamma}{K}\right),$$

where $N_\alpha$ is the abundance of species $\alpha$, $C_{\alpha,\beta}$ is the cooperativity coefficient, $K$ is the carrying capacity which is assumed to be $10^9$, and $b$ is the buffer term used for low-density growth which is assumed to be $10^5$. Fold-growth in pairwise co-cultures is used to fit $C_{\alpha,\beta}$, whose values are adjusted based on the gradient descent approach to minimize the difference between experimental data and model predictions. Eventually, the model with fitted $C_{\alpha,\beta}$ is used to generate the prediction for the 14-member co-culture result.

**Statistics.** All simulations and analyses were performed using standard numerical and scientific computing libraries in the Python programming language (version 3.7.1) and Jupyter Notebook (version 6.1).

**Data and code availability.** All code for simulations used in this manuscript can be found at `https://github.com/wt1005203/auxotroph`.


[1] G. D'Souza, S. Waschina, S. Pande, K. Bohl, C. Kaleta, and C. Kost, Evolution **68**, 2559 (2014).

[2] M. Embree, J. K. Liu, M. M. Al-Bassam, and K. Zengler, Proceedings of the National Academy of Sciences **112**, 15450 (2015).

[3] Y.-F. Liu, D. D. Galzerani, S. M. Mbadinga, L. S. Zaramela, J.-D. Gu, B.-Z. Mu, and K. Zengler, Microbiome **6**, 1 (2018).

[4] W. R. Harcombe, J. M. Chacón, E. M. Adamowicz, L. M. Chubiz, and C. J. Marx, Proceedings of the National Academy of Sciences **115**, 12000 (2018).

[5] S. Starke, D. M. Harris, J. Zimmermann, S. Schuchardt, M. Oumari, D. Frank, C. Bang, P. Rosenstiel, S. Schreiber, N. Frey, *et al.*, The ISME Journal **17**, 2370 (2023).

[6] J. A. Metz, S. A. Geritz, G. Meszéna, F. J. Jacobs, and J. S. Van Heerwaarden, (1995).

[7] B. Momeni, L. Xie, and W. Shou, Elife **6**, e25051 (2017).

[8] M. T. Mee, J. J. Collins, G. M. Church, and H. H. Wang, Proceedings of the National Academy of Sciences **111**, E2149 (2014).

[9] M. Raatz, Peer Community Journal **3** (2023).

[10] M. N. Guillen, B. Rosener, S. Sayin, and A. Mitchell, Cell Systems **12**, 1064 (2021).

[11] R. MacArthur, Theoretical population biology **1**, 1 (1970).

[12] R. Marsland III, W. Cui, J. Goldford, A. Sanchez, K. Korolev, and P. Mehta, PLoS computational biology **15**, e1006793 (2019).

[13] T. Okayasu, M. Ikeda, K. Akimoto, and K. Sorimachi, Amino Acids **13**, 379 (1997).

[14] H. Akashi and T. Gojobori, Proceedings of the National Academy of Sciences **99**, 3695 (2002).

[15] E. M. Heizer Jr, D. W. Raiford, M. L. Raymer, T. E. Doom, R. V. Miller, and D. E. Krane, Molecular biology and evolution **23**, 1670 (2006).

[16] C. You, H. Okano, S. Hui, Z. Zhang, M. Kim, C. W. Gunderson, Y.-P. Wang, P. Lenz, D. Yan, and T. Hwa, Nature **500**, 301 (2013).

[17] M. Zampieri, M. Hörl, F. Hotz, N. F. Müller, and U. Sauer, Nature communications **10**, 1 (2019).

[18] M. Dougoud, L. Vinckenbosch, R. P. Rohr, L.-F. Bersier, and C. Mazza, PLoS computational biology **14**, e1005988 (2018).

[19] R. M. May, Nature **238**, 413 (1972).

[20] S. Allesina and S. Tang, Nature **483**, 205 (2012).

[21] V. Dubinkina, Y. Fridman, P. P. Pandey, and S. Maslov, Elife **8**, e49720 (2019).

[22] D. Tilman, *Resource competition and community structure*, 17 (Princeton university press, 1982).

[23] A. Posfai, T. Taillefumier, and N. S. Wingreen, Physical review letters **118**, 028103 (2017).

[24] K. J. Kauffman, P. Prakash, and J. S. Edwards, Current opinion in biotechnology **14**, 491 (2003).

[25] J. D. Orth, I. Thiele, and B. Ø. Palsson, Nature biotechnology **28**, 245 (2010).


**Acknowledgements.** We thank Veronika Dunbinka and Zihan Wang for useful discussion.

**Author contributions.** All authors helped devise the study; TW performed the research and analyzed the data; SM supervised the research; TW and SM wrote the manuscript.

**Competing Interests.** The authors declare no competing interests.